ChemPhysChem

Research Article
doi.org/10.1002/cphc.202300001

Chemistry Europe
European Chemical Societies Publishing

www.chemphyschem.org

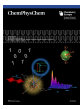

Observation of a Long-lived Electronic Coherence Modulated by Vibrational Dynamics in Molecular Nd^{3+}-Complexes at Room Temperature

Jayanta Ghosh,[a] Mirali Gheibi,[a] Tillmann Kalas,[a] Cristian Sarpe,[a] Bastian Zielinski,[a] Ramela Ciobotea,[a] Christoph Burghard Morscher,[a] Ingo Koehne,[b] Rudolf Pietschnig,[b] Arne Senftleben,[a] Thomas Baumert,[a] and Hendrike Braun*[a]

Temporally delayed, phase-locked coherent pairs of near IR femtosecond laser pulses were employed to study electronic coherences in molecular Nd^{3+}-complexes at room temperature. Dissolved and solid complexes were studied under a confocal microscope set-up with fluorescence detection. The observed electronic coherence on a few hundred femtoseconds time scale is modulated by additional coherent wave packet dynamics, which we attribute mainly to be vibrational in nature. In future, the complexes may serve as prototypes for possible applications in quantum information technology.

Introduction

Quantum information science[1,2] is based on the quantum superposition principle realised in qubits. Rigorous efforts are being made in the scientific community to find ideal quantum systems that are suitable as such. Experimentally, finding such ideal quantum systems is still challenging because of the major difficulties arising due to quantum decoherence, the loss of definite phase between quantum states. The other major challenge is the production of qubit systems on a large scale. To solve these two problems, nature already provides potentially ideal quantum systems in the form of molecules.[3] By using appropriate synthesis procedures, the production of most molecular complexes can be scaled up, making them interesting for quantum information.

Qubits are realised as coherent superpositions of states. The excitation of a level system like an atom with a femtosecond laser pulse in the IR can result in the coherent superposition of states with different characters. In the simplest case of a two-level system, an electronic coherence is created when the electronic ground and the electronically excited state are partially populated after interaction with the laser pulse. Expanding to a multi-level system, if more than one state in the excited state manifold gets populated due to the broad spectrum of the exciting laser pulse, an electronic wave packet is launched. Such states in the excited state manifold may be different electronic states or, for example, fine-structure states. In molecules, an additional possibility for the excitation of a coherent superposition arises: the excitation of a vibrational wave packet. The vibrational states participating in that superposition are determined by the bandwidth and the intensity distribution of the laser pulse and the Franck-Condon factors between the ground state and the energetically accessible target states. All these coherent wave packets exhibit a temporal evolution governed by the energy differences of the participating states. The electronic coherence between ground and excited state shows a beating with the Bohr-frequency, i.e. the frequency of the transition. For electronic as well as vibrational wave packets created in the excited state manifold, the beating frequency is given by the energy difference of the states coupled over the spectral bandwidth of the laser pulse. In molecular systems, the interaction with a laser pulse of broad spectral bandwidth can result in the creation of combinations of electronic and vibrational coherences. In this case, the signature of the electronic coherence between ground and excited state will be modulated. The temporal evolution of an electronic wave packet in the excited state would be reflected in an amplitude modulation of the electronic coherence signal in analogy to the modulation of ionisation probabilities for electronic fine structure wave packets.[4–6] The amplitude modulation of the electronic coherence signal by a vibrational wave packet would be due to the motion of the wave packet and the resulting loss and regaining of Franck-Condon overlap.[7–11]

Coherences, as described above in atoms and molecules in the gas phase, have been studied regarding their use in quantum information. Vibrational and rovibrational wave packets have been used to demonstrate the implementation of

[a] Dr. J. Ghosh, M. Gheibi, Dr. T. Kalas, C. Sarpe, B. Zielinski, R. Ciobotea, C. Burghard Morscher, Dr. A. Senftleben, Prof. Dr. T. Baumert, Dr. H. Braun
Institute of Physics and Center for Interdisciplinary Nanostructure Science and Technology (CINSaT), University of Kassel
Heinrich-Plett-Str. 40, 34132 Kassel, Germany
E-mail: braun@physik.uni-kassel.de
[b] Dr. I. Koehne, Prof. Dr. R. Pietschnig
Institute of Chemistry and Center for Interdisciplinary Nanostructure Science and Technology (CINSaT), University of Kassel
Heinrich-Plett-Str. 40, 34132 Kassel, Germany

Supporting information for this article is available on the WWW under https://doi.org/10.1002/cphc.202300001

universal quantum gates[12] while a Deutsch-Josza algorithm was implemented using rovibrational states in Li_2.[13] In terms of quantum storage on an atomic level employing electronic states, information about a flipped phase was stored in and read out of atomic Rydberg wave packets using a search algorithm.[14–16] The combination of different coherences may provide an additional reservoir for quantum information.

The use of coherences for quantum information requires their manipulation. With phase-shaped femtosecond laser pulses, this has been demonstrated for electronic coherences in atoms, molecules (here with the additional coupling of electronic and nuclear degrees of freedom) and semiconductor nanocrystals. For bandwidth-limited (BWL) pulses of 25 fs duration, pulse shaping was employed for tailoring the pulses to manipulate transient dynamics and final state populations on a one hundred femtosecond time scale.[4,17–21] This paves the way to implement quantum logic gates.

Regardless of the type of coherence, a major challenge is decoherence, the loss of definite phase between the participating quantum states. In general, electronic coherences in large molecular complexes are usually short-lived.[22] Electronic dephasing times are typically a few tens of femtoseconds.[23] In particular, the coherence time of electronic excitations in light-harvesting biomolecular complexes[24] has been studied. Recently, the unusually long lifetime of an electronic coherence of ca. 150 fs was measured in a single $CsPbBr_3$ perovskite quantum dot, whereas for non-perovskite quantum dots at room temperature coherence times in the tens of femtoseconds range are observed (e.g. 75 fs in colloidal CdSe).[25] In solutions of dye molecules, coherent third-order response was measured up to 180 fs.[26] Especially in a solution at room temperature, the interaction with the solvent molecules leads to these short lifetimes of the electronic coherence, while at a lower temperature, one might expect an increase of the lifetime.

Our study focuses on the electronic coherence created between the ground and the electronically excited state in Nd ions embedded into a molecular complex using near-IR femtosecond laser pulses. The molecular Nd^{3+}-complexes are particularly interesting candidates[27] for several reasons. Lanthanide ions pose discrete energy levels, and their 4*f* energy levels and electronic states are influenced to a significantly lower extent by the field of surrounding ligands than related d-block metals. Some lanthanide ions show prominent absorption around 800 nm, which is suitable for excitation with widely available Ti:Sapphire femtosecond laser systems.[28] The molecular Ln^{3+}-complexes can be tailored to be available for surface immobilisation and to provide sufficient rigidity beneficial for long-lived electronic states. Here we present our findings in condensed phase – solid and solution state – at room temperature. We discuss the lifetime of the electronic coherence, and its modulations by the simultaneous excitation of different superpositions. Despite the relative isolation of the 4*f* energy levels, we do not expect to observe the behaviour of an electronic coherence in a pure level system but to see an influence of molecular dynamics. We employ temporally delayed, phase-locked coherent pairs of pulses and fluorescence detection under a confocal microscope. In principle, in the perturbative interaction regime, analogue results could be obtained by Fourier transform spectroscopy or even using incoherent light.[29] However, the use of coherent pulses allows for controlling these electronic superpositions via different coherent control techniques in the non-perturbative regime.[30]

In this study we evaluated neodymium complexes $[Nd(L)_3A_3]$ (L = diisopropyl (4-bromobenzyl) phosphonate or 4-BrBzP(O)(O*i*Pr)$_2$; A=Cl^- or NO_3^-) carrying two different counterions (Figure 1a). The $[NdL_3(NO_3)_3]$ complex exists in monomeric form, the $[NdL_3Cl_3]_2$ complex in dimeric form. In the following, the chloride-containing complex $[Nd(L)_3Cl_3]_2$ is abbreviated as $NdCl_3$-complex and the nitrate-containing complex $[Nd(L)_3(NO_3)_3]$ as $Nd(NO_3)_3$-complex. For details on the synthesis and characterisation of these two compounds, the reader is referred to the work of Pietschnig and coworkers.[31] These molecular complexes show a strong absorption around 800 nm which has a significant overlap with the spectrum of femtosecond laser pulses from Ti:Sapphire lasers. The overlap between the absorption spectra of the corresponding molecules and our laser spectrum is depicted in Figure 1(b). The strong absorption around 800 nm excites the Nd^{3+} system from the ground state ($^4I_{9/2}$) to the electronically excited manifolds $^4F_{5/2}$ and $^2H_{9/2}$.[28,31] However, $^4F_{5/2}$ and $^2H_{9/2}$ are not degenerate states but close in energy and can be accessed by the bandwidth of the excitation laser. We observe fluorescence emission from 870 nm to 910 nm (see Figure 1(c)). The fluorescence spectra contain two prominent bands (maxima of the bands around ~871 nm and ~905 nm) at room temperature. This emission was assigned to the radiative decay from the excited state $^4F_{3/2}$ to the manifold of the ground state $^4I_{9/2}$.[28,31] The overall excitation and emission scheme of the molecular Nd^{3+}-complexes is shown in Figure 1(d). The emission of the $Nd(NO_3)_3$-complex around 871 nm shows a small blue shift (~7 nm) in comparison to the $NdCl_3$-complex. The detected fluorescence from the dissolved and solid $Nd(NO_3)_3$-complex shows maxima at the same wavelengths. We could not detect any fluorescence from a solution of the $NdCl_3$-complex.

Experimental Setup

Figure 2 depicts the schematic experimental set-up. A femtosecond laser, a pulse shaper, a confocal microscope, and a spectrometer construct the main parts of the set-up. This layout is applied initially to detect the lanthanide complexes' fluorescence signal in both liquid and solid phases. Afterwards, it is used to implement pump-probe measurements to study the electronic coherence in the complex. A Ti:Sapphire femtosecond laser (Femtosource/Scientific XL) generates pulses with a central wavelength of 795 nm, a repetition rate of 5.1 MHz, and a pulse duration of 38 fs (SI, Figure S3). In the pulse shaper, two parallel liquid crystal-spatial light modulators (LC-SLMs) with 640 pixels each (Jenoptik SLM–S640d) are mounted perpendicular to the beam in the Fourier plane of the 4f set-up. The LC-SLMs have orientation axes of $\pm 45°$ and allow for independent modulation of the spectral phase of both polarisation components of the incoming laser pulses. We employ Phase Resolved Interferometric Spectral Modulation (PRISM) to determine the spectral phase for compensating the optical dispersion under the microscope objective.[32] In the described experiments, this compensation phase is always applied to the LC-

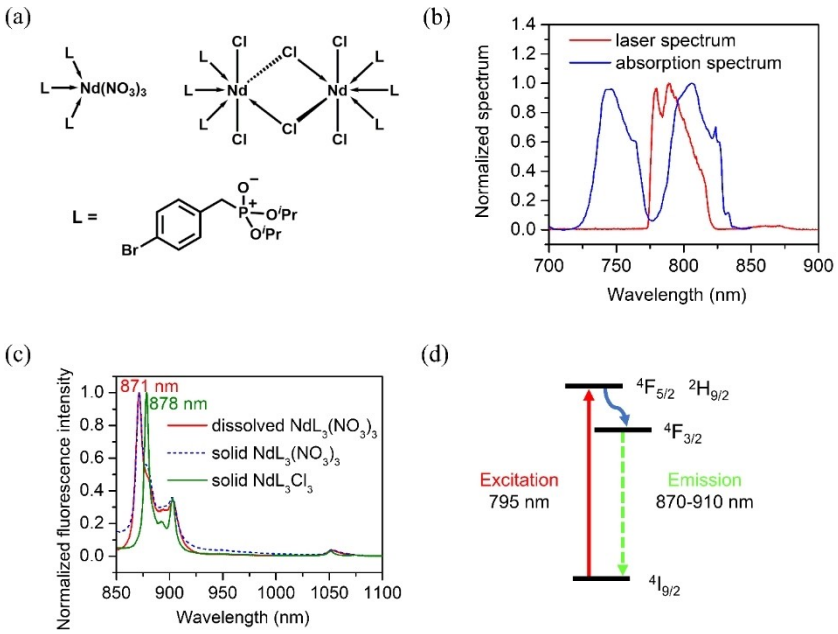

Figure 1. (a) Chemical structure of the two Nd^{3+}-complexes (left: $Nd(NO_3)_3$-complex in monomeric form, right: $NdCl_3$-complex in dimeric form), (b) laser spectrum (red) and absorption spectrum of Nd^{3+}-complexes (blue)[31] in the overlap region, (c) fluorescence observed after excitation with near-IR femtosecond laser pulses for the solution (red) and the solid $Nd(NO_3)_3$-complex (dotted blue) and the solid $NdCl_3$-complex (green), (d) schematic diagram of the excitation (red) and subsequent relaxation (blue) and emission (green) processes in the molecular Nd^{3+}-complexes (Note that $^4F_{5/2}$ and $^2H_{9/2}$ are not degenerate states, the depiction of only three levels is a simplification, chosen for easy explanation).

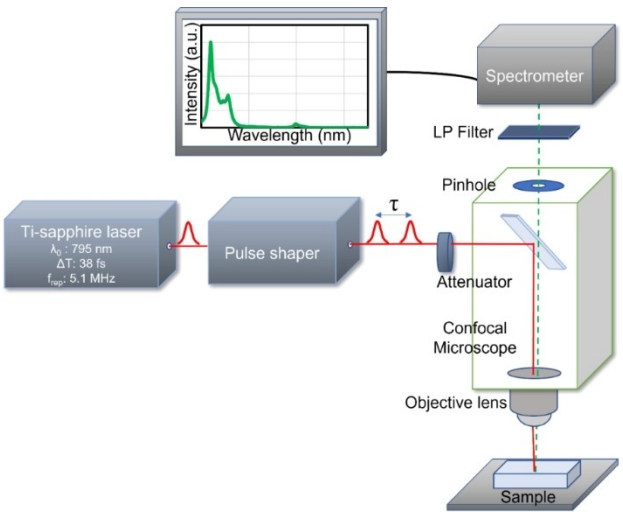

Figure 2. Experimental set-up for investigating electronic coherence via fluorescence detection containing laser system, pulse shaper, confocal microscope, and spectrometer.

SLMs to ensure bandwidth-limited (BWL) pulses at the point of the laser excitation. The laser pulses passing through the pulse shaper and the confocal microscope excite the lanthanide complexes. The scattered light and the fluorescence from the sample are collected via the objective lens and are directed through a confocal pinhole to a spectrometer (Andor DB401_UV) as the detector. Filtering the detected light before the spectrometer using a long-pass filter (LP filter, for details see SI, section 6) enables us to detect only the fluorescence region of the spectrum by significantly blocking the laser spectral region. The coherent pair of BWL pulses, as required for the pump-probe measurements to study the electronic coherence, are generated by our pulse shaper. Independent phase-shaping of two polarisation components enables us to control the delay-time of the pair of pulses with zeptosecond precision.[33] To measure the evolution of the electronic coherence, each coherent pair of pulses can be considered as a sequence of pump and probe pulses. The first pulse induces a superposition of electronic states – an electronic coherence that will persist after the pump pulse has ended. The electronic coherence's evolution is governed by the energy difference of the participating states. When the second pulse interacts with the persisting coherence after a well-defined delay-time, it probes the coherence in a phase-sensitive manner, leading to an enhancement or a decline in the population of the upper electronic state. In this, the coherent pair of pulses is similar to the first two pulses employed in coherent 2D spectroscopy.[34] The delay-time dependent change in the population results in a delay-time dependent modulation of the subsequent fluorescence recorded by the spectrometer. Fluorescence spectra are taken for delay-times between −150 fs and 1200 fs. We took three accumulation cycles with 100 ms acquisition time for each measurement.

Eventually, the detected spectra for all delay-times are recorded in a data file. We performed coherent pair of pulses experiments at two different average laser powers that correspond to a peak intensity of each individual pulse of $I_0 = 1.95 \times 10^{11}$ W/cm^2 and $3I_0 = 5.85 \times 10^{11}$ W/cm^2, respectively.

For data analysis, the spectrum for each delay-time (Figure 3 (a)) is integrated over the fluorescence region (860 nm–920 nm, marked by horizontal dashed lines). The integrated signal (Figure 3 (b)) shows delay-time dependent modulations. In the region of optical overlap of the two pulses, these modulations are due to optical interferences (cf. inset in (b) from 0 to 20 fs). For larger delay times (> 300 fs), the modulations are due to quantum mechanical interferences (cf. insets from 360 fs to 380 fs and 590 fs to 610 fs). The interferences in both regions show the same frequency as the

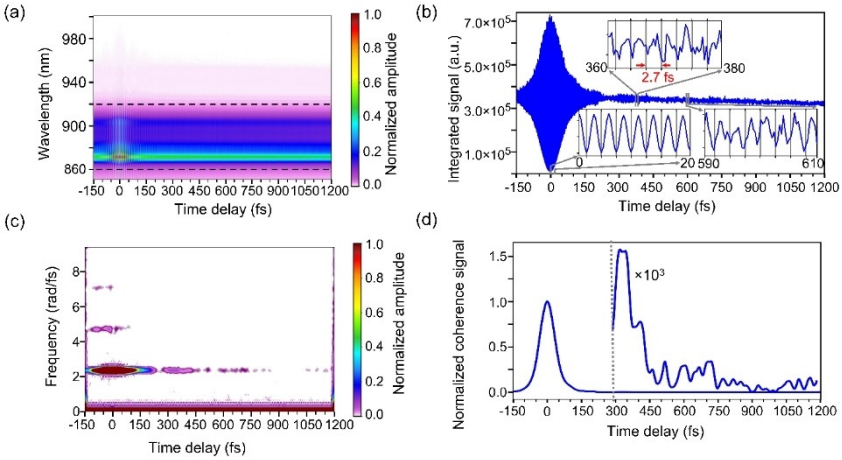

Figure 3. Data processing steps used to analyse the electronic coherence induced in the Nd^{3+}-complexes (data from 0.1 mol/l solution of $Nd(NO_3)_3$-complex measured at peak pulse intensities of I_0). (a) Fluorescence spectra after interaction with coherent pairs of pulses for delay-times from −150 fs to 1200 fs, dashed lines indicate the relevant fluorescence region, (b) spectra from (a) integrated for each delay-time over the fluorescence region, insets in (b) visualise the delay-time dependent modulation of the integrated fluorescence signal, 0 fs to 20 fs is a zoom into the region of optical interferences, while 360 fs to 380 fs and 590 fs to 610 fs are exemplary zooms into the region of quantum mechanical interferences. Vertical lines indicate a period of 2.7 fs corresponding to 2.356 rad/fs, (c) STFT of integrated signal in (b), (d) trace of the 2.356 rad/fs signal from (c). For delay-times larger than 288 fs, a scaling factor is used for better visibility.

excitation is done resonantly. We then perform a Short Time Fourier Transform (STFT) of the integrated signal, which reveals the delay-time dependent frequency contributions to the fluorescence signal (Figure 3(c)). For details on the STFT see SI, section 5. The electronic excitation from the ground to the excited state of the Nd^{3+} ion is driven by our 795 nm laser pulses corresponding to a frequency of ~2.356 rad/fs. Therefore, we interpret the STFT signal at this frequency (plotted in Figure 3(d)) as the signature of the induced electronic coherence.[35] Regular modulations of this STFT signal point to the simultaneous excitation of additional electronic or vibrational coherences in the excited state manifold. The duration over which this 2.356 rad/fs component of the fluorescence signal can be observed corresponds to the time over which the electronic coherence is detectable. Additional signals around 4.731 rad/fs and 7.069 rad/fs around a time delay of 0 fs in Figure 3(c) are artefacts of the evaluation.

The Nd^{3+}-complexes for our measurements (Figure 1(a)) are provided in solid form. We performed our experiments in this aggregate state and, in addition, in dissolved state to ensure close to single molecule response and to avoid crystalline effects. To prepare the samples for our experiments, the solid Nd^{3+}-complexes were put on glass slides. The samples were covered by coverslips (glass, thickness 0.16 mm), which were glued shut for sealing. 0.1 and 0.05 mol/l solutions of the $Nd(NO_3)_3$-complex were produced by dissolving in dry dichloromethane (dry-DCM). To detect the fluorescence of the dissolved sample, the prepared solution of the $Nd(NO_3)_3$-complex was transferred to a thin 1 mm optical path length quartz cuvette. The cuvette was placed with the focal plane of the objective lens of the microscope well within the liquid. Similarly, for the solid molecular complexes, the samples between the glass slides were placed at the focal plane of the objective lens.

Results and Discussion

As a first step, we recorded single pulse fluorescence spectra of the Nd^{3+}-complexes after interaction with 795 nm femtosecond laser pulses from the solid and dissolved samples Afterwards, we studied the electronic coherence in the samples by performing coherent pair of pulses measurements at different excitation powers and in the case of the solution with different concentrations.

The fluorescence from both dissolved and solid samples was stable throughout our measurement; we did not observe any significant bleaching of the fluorescence signal. After measurement of the single pulse fluorescence spectra (Figure 1(c)), we employed pairs of femtosecond laser pulses with varying time delays created by our pulse shaper to study the electronic coherence via the recorded fluorescence. The interaction of the molecular system with the first pulse of a pulse pair creates a coherent superposition between ground and excited state. When the second pulse arrives, depending on the phase difference between the second pulse and the induced coherence, the population of the upper state can be enlarged or reduced because of constructive or destructive interference. This delay-time dependent change in population is reflected in the subsequent fluorescence as a periodic modulation of the signal. The modulation of the delay-time dependent fluorescence signal at 2.356 rad/fs (period of ~2.7 fs) is the measure of the coherent superposition between ground and excited electronic state. The excitation from ground state ($^4I_{9/2}$) to the excited state ($^4F_{5/2}$ and $^2H_{9/2}$) by a pulse of a central wavelength of 795 nm gives rise to the beating at 2.7 fs which is the fingerprint of electronic coherence. For temporal overlap of the pulses (< 300 fs to account for low intensity wings of the pulses), the observed modulation in the fluorescence signal is due to optical interferences also with a period of 2.7 fs. At larger delay-times, the observed modulations are purely due to the described quantum mechanical interferences.

In the first experiment, fluorescence signals were recorded from the 0.1 mol/l $Nd(NO_3)_3$-complex solution and the solid complex for temporal separations of the pump and probe pulse

between −150 fs and 1200 fs with a step size of 0.33 fs. The STFT of the integrated fluorescence signal shows a long-lived coherence signal for both dissolved and solid $Nd(NO_3)_3$-complex (Figure 4(a) and (b)). The modulations of the coherence signal can be observed up to 1 ps and are shown in Figure 4(c) and (d). They are visible for several different measurement conditions, confirming the reproducibility and robustness of our measurements.

To check the power dependence of the coherence signal, we carried out a coherent pair of pulses measurement under the same conditions at $3I_0$ with the same concentration (0.1 mol/l) of the dissolved $Nd(NO_3)_3$-complex. The amplitude of the fluorescence signal (Figure S1(a)) grows by a factor of 2.8 when the peak intensity is increased (from I_0 to $3I_0$) which confirms the measurements are done in the linear regime. The comparison of the temporal evolution of the coherence signal for the two excitation powers beyond the optical overlap region (Figure 4(c), red and black) shows a nearly identical modulation.

Furthermore, we tested the concentration dependence of the signal in the linear excitation regime by performing a coherent pair of pulses measurement with two different concentrations (0.1 mol/l and 0.05 mol/l) of the $Nd(NO_3)_3$-complex solution at the same peak pulse intensity (I_0). The amplitude of the fluorescence signal varies linearly (50 %) when changing the concentration (50 %) of the solution (Figure S1(b)), while the temporal evolution of the coherence signal remains similar for the two different concentrations (Figure 4(c), 0.1 mol/l in red and 0.05 mol/l in cyan).

Likewise, the temporal evolution of the coherence signal from the solid $Nd(NO_3)_3$-complex at two different peak pulse intensities (I_0 and $3I_0$) shows similar behaviour (Figure 4(d)).

In addition to measurements with the $Nd(NO_3)_3$-complex, we studied the electronic coherence and its decay for the solid $NdCl_3$-complex. The temporal evolution of the coherence signal from the solid $NdCl_3$-complex is depicted in the Supporting Information (Figure S2(b)). For the solid $NdCl_3$-complex, the coherence signal shows a larger amplitude as compared to both the solid and the dissolved sample of the $Nd(NO_3)_3$-complex (Figure S2(a)).

To compare with the coherence signals observed from the Nd^{3+}-complexes, we checked the 2.356 rad/fs contribution of a first-order autocorrelation of the femtosecond laser pulses measured with a photodiode at the position of the sample. (Figure S2(a) and S2(b)). For the first-order autocorrelation, the 2.356 rad/fs contribution originates purely from optical interference and can be observed up to 200 fs. We observe no correlation between this signal and the coherence signal from the samples. Moreover, in the region up to 1 ps, the coherence signal has a significantly higher amplitude than the purely optical signal.

In Figure 4(c) and 4(d), the coherence signals from the Nd^{3+}-complexes exhibit additional modulations. This behaviour can be expected for a molecular system (cf. Introduction) and originates in the simultaneous excitation of coherent superpositions in addition to the electronic coherence between ground and excited state. In the case of the dissolved $Nd(NO_3)_3$-complex, the modulation shows roughly a period of 150 fs which can be observed up to 1 ps. The modulation does not appear as regular for the solid $Nd(NO_3)_3$-complex. The period of 150 fs corresponding to an energy difference of 27.6 meV (222.4 cm^{-1}, 6.67 THz) is not compatible with level spacings of next neighbour *electronic* states in the $^4F_{5/2}$ and $^2H_{9/2}$ states of Nd^{3+} reported in the literature: The largest energy difference between electronic states in Nd^{3+}-complexes ($^4F_{5/2}$ and $^2H_{9/2}$) is 11.2 meV (90.4 cm^{-1}, ~2.7 THz) resulting in a 370 fs beating period.[36–38] An electronic coherence in the excited states of the Nd^{3+}-complexes used in this study would show up with a beating period of 370 fs or longer. Hence, we attribute the modulation of the electronic coherence signal to the excitation of a *vibrational* coherence resulting in vibrational wave packet motion. In this case, the amplitude modulation of the electronic coherence signal would be due to the resulting loss and regaining of Franck-Condon overlap.[7–11] Initial attempts to influence the vibrational wave packet by reducing the width

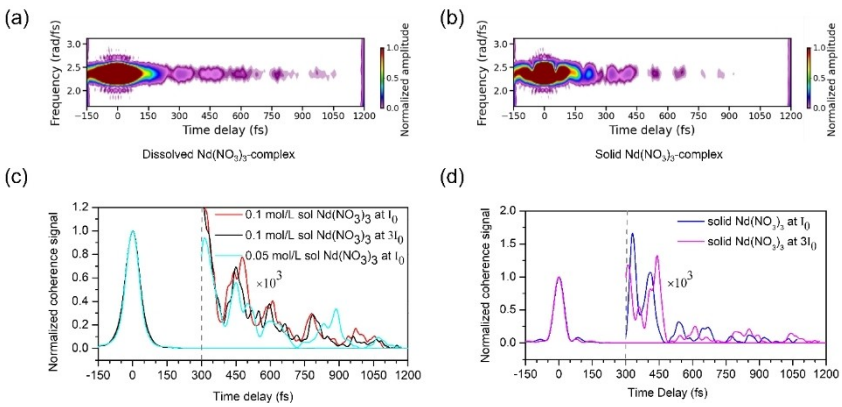

Figure 4. (a) STFT of integrated fluorescence spectra obtained by pump-probe measurements from dissolved $Nd(NO_3)_3$-complex (concentration: 0.1 mol/l) at I_0, (b) from solid $Nd(NO_3)_3$-complex at I_0 and (c) normalized coherence signal from dissolved $Nd(NO_3)_3$-complex by varying concentrations and peak pulse intensities: 0.1 mol/l concentrated solution at I_0 (red), 0.1 mol/l concentrated solution at $3I_0$ (black), and 0.05 mol/l concentrated solution at I_0 (cyan) (scaled 2.356 rad/fs signal) and (d) solid $Nd(NO_3)_3$- complex at two different peak pulse intensities: I_0 (blue) and $3I_0$ (magenta) (scaled 2.356 rad/fs signal).

and the centre of the excitation spectrum have not been conclusive yet (Figure S4).

In the case of the $NdCl_3$ -complex, the coherence signal seems to exhibit an additional frequency component with a period of around 450 fs (Figure S2(b)). This frequency component of 2.22 THz (~74 cm^{-1}) could be attributed to another, simultaneously excited coherence, which would correspond to an energy difference of 9 meV. Such an energy difference, corresponding to a period of 450 fs, might be found between the above-mentioned participating electronic states in the excited-state manifold of Nd^{3+}. Hence, for the $NdCl_3$-complex we cannot exclude electronic contributions to the observed modulations of the coherence signal. Via 2D-spectroscopy it is, in principle, possible to determine the character of the observed wave packets (vibrational or electronic).[39]

For the estimation of the lifetime of the electronic coherence, we fitted a single exponential decay function ($y = y_0 + Ae^{-x/t}$) to the observed modulations of the electronic coherence signals depicted in Figure 4(c) and (d) for solvated 0.1 mol/l and solid $Nd(NO_3)_3$-complexes. We used data points for delay-times larger than 300 fs to exclude the region of optical interferences. The fitting results are lifetimes of around 324 fs for the 0.1 mol/l $Nd(NO_3)_3$-complex solution and around 141 fs for the solid $Nd(NO_3)_3$-complex. A similar lifetime (~156 fs) was also found in case of the solid $NdCl_3$-complex. We attribute the longer lifetime of the electronic coherence in solution compared to that of solid Nd^{3+}-complexes to the fact that the molecules are less influenced by neighbour molecules in solutions than in the solid phase. Overall, we observed lifetimes of the electronic coherence in the range of a few hundred femtoseconds.

The focus of the presented pump-probe measurements is to determine the lifetime of the electronic coherence, its modulation by the simultaneous excitation of different superpositions and how long its signature persists. In our measurements with Nd^{3+}-complexes, we can clearly observe the signature of the electronic coherence beyond the optical interference region up to 1 ps with a lifetime around 324 fs to 141 fs for solutions (Figure 5(a)) and the solid $Nd(NO_3)_3$-complex (Figure 5(b)), respectively. This long-lived electronic coherence has been observed both in the dissolved (Figure 4(a, c)) and the solid $Nd(NO_3)_3$-complex (Figure 4(b, d)) as well as in the $NdCl_3$-complex (Figure S2(b), green). In the linear regime, the signal of the electronic coherence does not depend on the laser power (Figure 4(c), red and black curve and Figure 4(d), blue and magenta curve) or the concentration of the solutions (Figure 4(c), red and cyan curve). Furthermore, the long lifetime of the observed electronic coherence is comparable for both the nitrate- and the chloride-based Nd-complex under discussion, despite significant structural differences in terms of complex-nuclearity (monomeric, $[NdL_3(NO_3)_3]$ or dimeric, $[NdL_3Cl_3]$) and Nd···Nd distances (shortest Nd···Nd contact: 11.0 Å, $[NdL_3(NO_3)_3]$ vs. 4.8 Å, $[NdL_3Cl_3]$) based on single crystal X-ray diffraction. The electronic coherence is robust with respect to structure, aggregation state and concentration effects. The 4*f* states of neodymium, participating in excitations in the near-IR, are influenced to a significantly lower extent by the field of surrounding ligands than related d-block metals. It can be anticipated that this feature at least contributes to the extraordinary lifetime of the optically induced electronic coherence. For the $Nd(NO_3)_3$-complex, a modulation of the coherence signal is attributed to the creation of a vibrational coherence in the excited electronic state. In the case of the $NdCl_3$-complex, an additional modulation on top of a vibrational coherence shows up that may originate from an electronic wave packet launched in the excited state manifold. Both modulations, due to the vibrational or the additional electronic coherence, show a different frequency than the modulation of the fluorescence signal originating from the electronic coherence between ground and excited state.

Summary and Outlook

The long-lived electronic coherence induced by the excitation with 795 nm femtosecond laser pulses has been explored in molecular Nd^{3+}-complexes with different anions in solution and solid state at room temperature. We employed phase-stable coherent pairs of pulses as pump and probe pulses to induce and interrogate the coherence. Its signature, observed as a periodic modulation of the fluorescence signal dependent on the temporal delay within the coherent pair of pulses, persists up to 1 ps both in solid Nd^{3+}-complexes and their solutions. With respect to the usually short lifetime of electronic coherences, our observation of a persisting long-lived electronic coherence with a lifetime of a few hundred femtoseconds in Nd^{3+}-complexes at room temperature is remarkable and very promising. The additional modulations in the observed coherence signal are attributed to the creation of electronic or

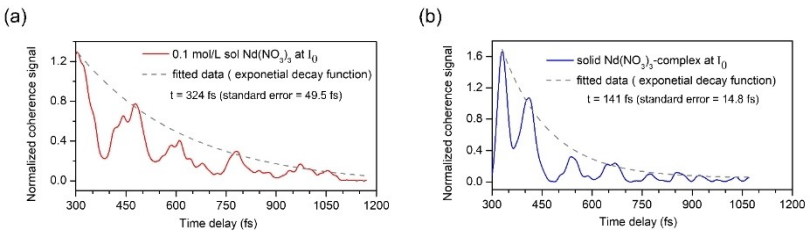

Figure 5. Scaled normalised coherence signal from (a) dissolved $Nd(NO_3)_3$-complex measured at I_0 (red) and fitted single exponential decay function (grey) and (b) solid $Nd(NO_3)_3$-complex measured at I_0 (blue) and fitted single exponential decay function (grey).

vibrational wave packets in the excited states or a combination, which may provide an additional reservoir for quantum information. The long-lived electronic coherence may open the door to investigate the implementation of quantum gates through ultrafast coherent control using phase-shaped femtosecond laser pulses.

Author contributions

J.G. and M.G. conducted the experiment and analysed the data; T.K. and B.Z. assisted the data acquisition; C.S. and R.C. helped with the maintenance of the experimental setup; I.K. and R.P. synthesised the chemical compounds. C.B.M. and all authors discussed the data. H.B., A.S., and T.B. contributed to developing the idea; J.G. wrote the manuscript with contributions from M.G., H.B., A.S., and T.B.; T.B. and A.S. helped supervision; H.B. supervised the project.

Acknowledgements

The federal state of Hesse, Germany, is kindly acknowledged for financial support of the SMolBits project within the LOEWE program. Open Access funding enabled and organized by Projekt DEAL.

Conflict of Interest

The authors declare no conflict of interest.

Data Availability Statement

The data that support the findings of this study are available from the corresponding author upon reasonable request.

Keywords: electronic coherence · femtochemistry · fluorescence · lanthanides · wave packets

[1] M. E. Flatté, I. Ţifrea, *Manipulating Quantum Coherence in Solid State Systems*, Springer Netherlands, Dordrecht, **2007**.
[2] D. D. Awschalom, L. C. Bassett, A. S. Dzurak, E. L. Hu, J. R. Petta, *Science* **2013**, *339*, 1174.
[3] C. M. Tesch, R. de Vivie-Riedle, *Phys. Rev. Lett.* **2002**, *89*, 157901.
[4] H. Braun, T. Bayer, D. Pengel, M. Wollenhaupt, T. Baumert, *J. Mod. Opt.* **2017**, *64*, 1042.
[5] S. Zamith, M. A. Bouchene, E. Sokell, C. Nicole, V. Blanchet, B. Girard, *Eur. Phys. J. D* **2000**, *12*, 255.
[6] V. Blanchet, C. Nicole, M. A. Bouchene, B. Girard, *Phys. Rev. Lett.* **1997**, *78*, 2716.
[7] N. F. Scherer, R. J. Carlson, A. Matro, M. Du, A. J. Ruggiero, V. Romero-Rochin, J. A. Cina, G. R. Fleming, S. A. Rice, *J. Chem. Phys.* **1991**, *95*, 1487.
[8] T. Baumert, J. Helbing, G. Gerber, in *Advances in Chemical Physics – Photochemistry: Chemical Reactions and their control on the Femtosecond Time Scale* (Eds.: I. Prigogine, S. Rice), John Wiley & Sons, Inc, New York, **1997**, pp. 47–77.
[9] C. Leichtle, W. P. Schleich, I. S. Averbukh, M. Shapiro, *J. Chem. Phys.* **1998**, *108*, 6057.
[10] M. Fushitani, *Annu. Rep. Prog. Chem. Sect. C* **2008**, *104*, 272.
[11] C. Menzel-Jones, M. Shapiro, *J. Phys. Chem. Lett.* **2012**, *3*, 3353.
[12] R. de Vivie-Riedle, U. Troppmann, *Chem. Rev.* **2007**, *107*, 5082.
[13] J. Vala, Z. Amitay, B. Zhang, S. R. Leone, R. Kosloff, *Phys. Rev. A* **2002**, *66*, 062316.
[14] J. Ahn, T. C. Weinacht, P. H. Bucksbaum, *Science* **2000**, *287*, 463.
[15] J. Ahn, D. N. Hutchinson, C. Rangan, P. H. Bucksbaum, *Phys. Rev. Lett.* **2001**, *86*, 1179.
[16] J. Ahn, C. Rangan, D. N. Hutchinson, P. H. Bucksbaum, *Phys. Rev. A* **2002**, *66*, 022312.
[17] T. Bayer, M. Wollenhaupt, C. Sarpe-Tudoran, T. Baumert, *Phys. Rev. Lett.* **2009**, *102*, 023004.
[18] T. Bayer, H. Braun, C. Sarpe, R. Siemering, P. von den Hoff, R. de Vivie-Riedle, T. Baumert, M. Wollenhaupt, *Phys. Rev. Lett.* **2013**, *110*, 123003.
[19] T. Bayer, M. Wollenhaupt, H. Braun, T. Baumert in *Advances in Chemical Physics* (Eds.: P. Brumer, S. A. Rice, A. R. Dinner), John Wiley & Sons, Inc, Hoboken, NJ, USA, **2016**, pp. 235–282.
[20] J. Schneider, M. Wollenhaupt, A. Winzenburg, T. Bayer, J. Köhler, R. Faust, T. Baumert, *Phys. Chem. Chem. Phys.* **2011**, *13*, 8733.
[21] M. Ruge, R. Wilcken, M. Wollenhaupt, A. Horn, T. Baumert, *J. Phys. Chem. C* **2013**, *117*, 11780.
[22] T. Buckup, J. Léonard in *Multidimensional Time-Resolved Spectroscopy*, (Eds.: T. Buckup, J. Léonard) Springer International Publishing, Cham, **2019**, pp. 207–245.
[23] J. Cao, R. J. Cogdell, D. F. Coker, H.-G. Duan, J. Hauer, U. Kleinekathöfer, T. L. C. Jansen, T. Mančal, R. J. D. Miller, J. P. Ogilvie, V. I. Prokhorenko, T. Renger, H. S. Tan, R. Templaar, M. Thorwart, E. Thyrhaug, S. Westenhoff, D. Zigmantas, *Sci. Adv.* **2020**, *6*, eaaz4888.
[24] H.-G. Duan, V. I. Prokhorenko, R. J. Cogdell, K. Ashraf, A. L. Stevens, M. Thorwart, R. J. D. Miller, *Proc. Natl. Acad. Sci. USA* **2017**, *114*, 8493.
[25] F. Ricci, V. Marougail, O. Varnavski, Y. Wu, S. Padgaonkar, S. Irgen-Gioro, E. A. Weiss, T. Goodson, *ACS Nano* **2021**, *15*, 12955.
[26] A. Konar, V. V. Lozovoy, M. Dantus, *J. Spectrosc. Dyn.* **2014**, *4*, 26.
[27] P. Goldner, A. Ferrier, O. Guillot-Noël, in *Handbook on the Physics and Chemistry of Rare Earths*, pp. 1–78.
[28] *Lanthanide Luminescence: Photophysical, Analytical and Biological Aspects*, Springer, **2010**.
[29] R. R. Jones, D. W. Schumacher, T. F. Gallagher, P. H. Bucksbaum, *J. Phys. B: At. Mol. Opt. Phys.* **1995**, *28*, L405–L411.
[30] V. Blanchet, M. A. Bouchène, B. Girard, *J. Chem. Phys.* **1998**, *108*, 4862.
[31] I. Koehne, A. Lik, M. Gerstel, C. Bruhn, J. P. Reithmaier, M. Benyoucef, R. Pietschnig, *Dalton Trans.* **2020**, *49*, 16683.
[32] T.-W. Wu, J. Tang, B. Hajj, M. Cui, *Opt. Express* **2011**, *19*, 12961.
[33] J. Köhler, M. Wollenhaupt, T. Bayer, C. Sarpe, T. Baumert, *Opt. Express* **2011**, *19*, 11638.
[34] P. Nuernberger, S. Ruetzel, T. Brixner, *Angew. Chem. Int. Ed.* **2015**, *54*, 11368.
[35] R. Mittal, R. Glenn, I. Saytashev, V. V. Lozovoy, M. Dantus, *J. Phys. Chem. Lett.* **2015**, *6*, 1638.
[36] F. Chen, M. Ju, G. L. Gutsev, X. Kuang, C. Lu, Y. Yeung, *J. Mater. Chem. C* **2017**, *5*, 3079.
[37] J. B. Gruber, D. K. Sardar, D. Johnson, R. M. Yow, C. H. Coeckelenbergh, A. S. Nijjar, *Polym. Int.* **2006**, *55*, 1007.
[38] H. Loro, D. Vasquez, G. E. Camarillo, H. Del Castillo, I. Camarillo, G. Muñoz, C. J. Flores, A. J. Hernández, S. H. Murrieta, *Phys. Rev. B* **2007**, *75*, 125405.
[39] V. Butkus, J. Alster, E. Bašinskaitė, R. N. Augulis, P. Neuhaus, L. Valkunas, H. L. Anderson, D. Abramavicius, D. Zigmantas, *J. Phys. Chem. Lett.* **2017**, *8*, 2344.

Manuscript received: January 2, 2023
Revised manuscript received: March 21, 2023
Accepted manuscript online: March 23, 2023
Version of record online: April 25, 2023